

Contribution from the Institut für Physikalische und Theoretische Chemie and Physikalisches Institut, Abt. II, University of Erlangen-Nürnberg, D-8520 Erlangen, West Germany, Chemistry Division, Bhabha Atomic Research Centre, Bombay 400 085, India, and School of Chemistry, University of New South Wales, Kensington, NSW 2033, Australia

The Discontinuous High-Spin (5T_2) \rightleftharpoons Low-Spin (1A_1) Transition in Solid Bis(1,10-phenanthroline-2-carbaldehyde phenylhydrazone)iron(II) Bis(tetrafluoroborate): Hysteresis Effects, Concurrent Crystallographic Phase Change, Entropy of the Transition, and Effect of Pressure

E. KÖNIG,*^{1a} G. RITTER,^{1b} S. K. KULSHRESHTHA,^{1a,c} J. WAIGEL,^{1b} and H. A. GOODWIN²

Received June 1, 1983

The discontinuous high-spin ($S = 2$, 5T_2) \rightleftharpoons low-spin ($S = 0$, 1A_1) transition in solid $[\text{Fe}(\text{phy})_2](\text{BF}_4)_2$ (phy = 1,10-phenanthroline-2-carbaldehyde phenylhydrazone) has been investigated by variable-temperature ${}^{57}\text{Fe}$ Mössbauer-effect, magnetic susceptibility, X-ray diffraction, and DSC measurements. The transition is associated with a crystallographic phase change and is essentially of first order. A hysteresis of width $\Delta T = 9$ K has been observed, the transition being centered at $T_c^\uparrow \approx 286$ K for increasing and at $T_c^\downarrow \approx 277$ K for decreasing temperature. The ground states involved are characterized, at the transition temperature T_c^\uparrow , by $\Delta E_Q({}^5T_2) = 0.71$ mm s⁻¹, $\delta^{57}\text{Fe}({}^5T_2) = +0.93$ mm s⁻¹ and $\Delta E_Q({}^1A_1) = 1.63$ mm s⁻¹, $\delta^{57}\text{Fe}({}^1A_1) = +0.29$ mm s⁻¹. The total area of Mössbauer absorption shows pretransitional effects and a pronounced discontinuity at T_c due to the difference in the recoil-free fraction of $\Delta f \approx 65\%$. Above and below T_c , $-\ln A_{\text{total}}$ is well reproduced within the high-temperature approximation ($\Theta_{{}^5T_2} = 130$ K for $T > 290$ K, $\Theta_{{}^1A_1} = 180$ K for $T < 272$ K; $M_{\text{Fe}} = 57$ au). The X-ray diffraction patterns for the 5T_2 and 1A_1 phases are characteristically different, and details of the hysteresis are indicative of domain formation by both the spin states. The enthalpy and entropy changes associated with the spin transition are $\Delta H = 24.2 \pm 1.0$ kJ mol⁻¹ and $\Delta S = 85.8 \pm 4.0$ J mol⁻¹ K⁻¹, respectively. The high-spin (5T_2) \rightarrow low-spin (1A_1) transformation may be similarly induced by application of a moderate pressure. The Mössbauer parameters $\Delta E_Q({}^1A_1)$ and $\delta^{57}\text{Fe}({}^1A_1)$ indicate that the transformed state is practically identical with the temperature-induced low-spin 1A_1 state.

Introduction

Temperature- or pressure-induced transitions of the type high spin (5T_2) \rightleftharpoons low spin (1A_1) are known to show either continuous or essentially discontinuous behavior.³⁻⁵ The nature of the *continuous* transitions has been studied recently for a significant number of iron(II) complexes.⁶⁻⁸ These transitions do not exhibit individual X-ray diffraction patterns for the two spin constituents, high-spin 5T_2 and low-spin 1A_1 . Rather, the line intensities of the observed pattern are independent of temperature but the interplanar spacings d_{hkl} show a continuous variation with temperature. The variation is characteristic for the volume change associated with the spin transition. The results are consistent with the formation of a random solid solution of the two spin isomers within the same lattice. It has been suggested^{6,7} that continuous type spin transitions are formed for compounds with weak cooperative interaction between the individual complexes and a wide distribution of the nuclei of the minority spin constituent. Consistent results are now available for the compounds $[\text{Fe}(\text{bts})_2(\text{NCS})_2]$, where bts = 2,2'-bi(5-methyl-2-thiazoline),⁶ $[\text{Fe}(4\text{-paptH})_2]\text{X}_2 \cdot 2\text{H}_2\text{O}$, X = ClO₄, BF₄, where 4-paptH = 2-((4-methyl-2-pyridyl)amino)-4-(2-pyridyl)thiazole,⁷ and $[\text{Fe}(\text{dppen})_2\text{Cl}_2] \cdot 2(\text{CH}_3)_2\text{CO}$, where dppen = *cis*-1,2-bis(diphenylphosphino)ethylene.⁸

Discontinuous high-spin (5T_2) \rightleftharpoons low-spin (1A_1) transitions are encountered for iron(II) complexes with a strong cooperative interaction between the individual complexes. In the

transition region, individual X-ray diffraction patterns for the two phases, high-spin 5T_2 and low-spin 1A_1 , are observed, their intensities being strongly temperature dependent. Due to the interaction, the transition is associated with a crystallographic phase change, which is responsible for the abrupt change of various physical properties and which may be triggering the spin transition. The results have been interpreted⁹ by a pronounced domain formation by both the minority and the majority phases. In general, hysteresis effects are also observed which are a consequence of the domain formation. The same general features have been encountered for a number of iron(II) complexes.⁹⁻¹² However, complications due to the incomplete nature of the transition, i.e. the observation of a residual fraction,¹³ particle size effects,¹⁴ sample inhomogeneity, and impurities, have been found for certain systems.

Various other spin transitions in compounds of iron(II) have been studied.⁵ Since the results that would permit definite conclusions concerning the nature of the involved spin transition are usually lacking, these systems are not considered in detail. It should be noted that the differentiation between the two possible types of spin transition is believed to be of general applicability. It is therefore of considerable interest to study additional systems that exhibit spin transitions of the continuous or the discontinuous type in order to test this proposition.

The iron(II) complex $[\text{Fe}(\text{phy})_2](\text{BF}_4)_2$ has been shown, on the basis of magnetic measurements and optical electronic spectra, to exhibit an abrupt high-spin (5T_2) \rightleftharpoons low-spin (1A_1) transition¹⁵ (phy = 1,10-phenanthroline-2-carbaldehyde phe-

- (1) (a) Institut für Physikalische und Theoretische Chemie, University of Erlangen-Nürnberg. (b) Physikalisches Institut, Abt. II, University of Erlangen-Nürnberg. (c) Bhabha Atomic Research Centre.
- (2) University of New South Wales.
- (3) H. A. Goodwin, *Coord. Chem. Rev.*, **18**, 293 (1976).
- (4) R. L. Martin and A. H. White, *Transition Met. Chem. (N.Y.)*, **4**, 113 (1968).
- (5) P. Gülich, *Struct. Bonding (Berlin)*, **44**, 83 (1981).
- (6) E. König, G. Ritter, S. K. Kulshreshtha, and S. M. Nelson, *J. Am. Chem. Soc.*, **105**, 1924 (1983).
- (7) E. König, G. Ritter, S. K. Kulshreshtha, and H. A. Goodwin, *Inorg. Chem.*, **22**, 2518 (1983).
- (8) E. König, G. Ritter, S. K. Kulshreshtha, J. Waigel, and L. Sacconi, *Inorg. Chem.*, **23**, 1241 (1984).

- (9) E. König, G. Ritter, W. Irlner, and H. A. Goodwin, *J. Am. Chem. Soc.*, **102**, 4681 (1980).
- (10) E. König, G. Ritter, W. Irlner, and S. M. Nelson, *Inorg. Chim. Acta*, **37**, 169 (1979).
- (11) E. König, G. Ritter, and W. Irlner, *Chem. Phys. Lett.*, **66**, 336 (1979).
- (12) E. König, G. Ritter, S. K. Kulshreshtha, and S. M. Nelson, *Inorg. Chem.*, **21**, 3022 (1982).
- (13) E. König, G. Ritter, and S. K. Kulshreshtha, *Inorg. Chem.*, **23**, 1144 (1984).
- (14) E. König, G. Ritter, S. K. Kulshreshtha, and N. Csatory, *Inorg. Chem.*, accompanying paper in this issue.
- (15) H. A. Goodwin and D. W. Mather, *Aust. J. Chem.*, **27**, 965 (1974).

nylhydrazone). In the present contribution, we report a more detailed analysis of the spin transition based on ^{57}Fe Mössbauer-effect and X-ray powder diffraction measurements.

Experimental Section

Materials. The phenylhydrazone was prepared directly by interaction of 1,10-phenanthroline-2-carbaldehyde with phenylhydrazine in ethanol. The preparation of the complex $[\text{Fe}(\text{phy})_2](\text{BF}_4)_2$ using natural iron was reported previously.¹⁵ For the enriched complex, a modified procedure was followed.

Preparation of $^{57}\text{Fe}(\text{phy})_2(\text{BF}_4)_2$. ^{57}Fe powder (0.029 g) was suspended in deaerated water (5 mL), and 1 M (exactly) hydrochloric acid (1.00 mL) was added to the suspension, which was then heated on the steam bath under an atmosphere of nitrogen until all the metal had dissolved (about 1 h). A suspension of 1,10-phenanthroline-2-carbaldehyde phenylhydrazone (0.3 g) in hot ethanol (8 mL) was then slowly added, and an intensely brown solution was obtained. Water (15 mL) was then added to the mixture, which was kept hot and then filtered. Sodium fluoroborate solution was carefully added to the hot filtrate while the sides of the vessel were scratched to induce crystallization. Dark brown crystals of the monohydrate of $[\text{Fe}(\text{phy})_2](\text{BF}_4)_2$ separated. These were collected after the mixture was allowed to cool to room temperature slowly, washed with a little ice-cold water, and dried in vacuo over P_2O_5 .

Upon recrystallization of this sample from hot acetone by the careful addition of ether the anhydrous complex was obtained. It was collected from the hot solution and dried in vacuo over P_2O_5 .

Methods. ^{57}Fe Mössbauer spectra were measured with a spectrometer consisting of a constant-acceleration electromechanical drive and a Nuclear Data ND 2400 multichannel analyzer operating in the multiscaling mode. The source used consisted of 50-mCi ^{57}Co in rhodium, the calibration being effected with a metallic iron absorber. All velocity scales and isomer shifts are referred to the iron standard at 298 K. For conversion to the sodium nitroprusside scale, add $+0.257 \text{ mm s}^{-1}$. Variable-temperature measurements between 80 and 330 K were performed by using a custom-made superinsulated cryostat, the temperature being monitored by means of a calibrated iron vs. constantan thermocouple and a cryogenic temperature controller (Thor Cryogenics Model E 3010-II). The temperature stability was about $\pm 0.05 \text{ K}$. In order to prevent a temperature gradient across the sample, multiple layers of superinsulation foil were applied, and only the central area of 0.5 cm diameter of the absorber was used to detect the transmitted γ rays. The Mössbauer spectra were least-squares fitted to Lorentzian line shapes, and the areas were corrected for the nonresonant background of the γ rays.

In order to perform ^{57}Fe Mössbauer-effect measurements under an applied pressure, a sample enriched to over 90% in the isotope ^{57}Fe was pressed between two disks of boron carbide, B_4C , with use of a tin metal gasket. The assembly was enclosed in a tempered steel chamber, and a constant pressure was applied with a calibrated hydraulic press. The sample was retained under the chosen pressure by a suitable locking device, and for measurements at variable temperatures, it was placed in a cryostat.

Magnetic susceptibility was measured by the Gouy method employing a calibrated Newport Instruments variable-temperature balance.

Measurements of X-ray powder diffraction were obtained with a Siemens counter diffractometer, the resulting pulses being stored in an Elscint MEDA 10 multichannel analyzer. The diffractometer was used in the mode of step scanning, the angular steps in 2θ values being 0.02 or 0.005°. $\text{Cu K}\alpha$ radiation was used. Measurements at variable temperatures were performed with an Oxford Instruments CF 108A flow cryostat and liquid nitrogen as coolant. The achieved temperature stability was $\pm 0.1 \text{ K}$.

Differential scanning calorimetry (DSC) was measured with a Perkin-Elmer DSC-1B apparatus. The aluminum pan used as the sample holder was loosely covered but not crimped in order to avoid the application of pressure to the sample. The sample temperature was varied between 200 and 340 K at a constant rate of 8 K min^{-1} for heating/cooling under a stream of nitrogen gas. The sensitivity of the instrument was 4 mcal s^{-1} , and indium metal was employed for the calibration.

Results

^{57}Fe Mössbauer Spectra. Thermal Hysteresis Effects. A large number of ^{57}Fe Mössbauer spectra have been recorded

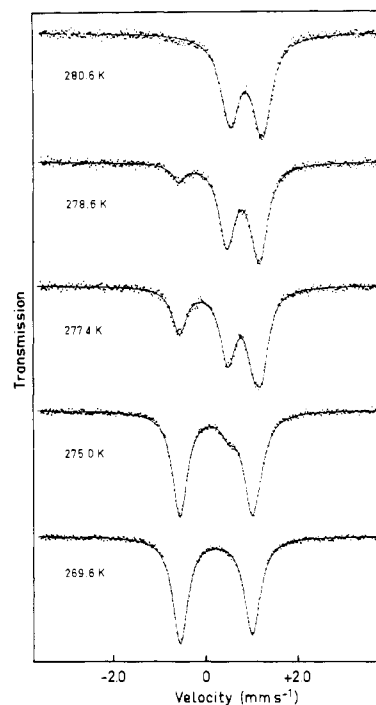


Figure 1. ^{57}Fe Mössbauer-effect spectra of an enriched sample of $[\text{Fe}(\text{phy})_2](\text{BF}_4)_2$ at 280.6, 278.7, 277.4, 275.0, and 269.6 K. The measurements were performed for decreasing temperatures ($T_c^\dagger \approx 277 \text{ K}$).

for samples of $[\text{Fe}(\text{phy})_2](\text{BF}_4)_2$ for both increasing and decreasing temperature sequences between 80 and 330 K. For a particular ^{57}Fe -enriched sample of the compound, Figure 1 shows five representative spectra in the spin transition region, i.e. those for 280.3, 278.6, 277.4, 275.0, and 269.6 K, selected from a decreasing-temperature series of measurements. It is apparent that, for this sample, the transition is complete at both extremes of this narrow temperature range. The lone doublet in the spectrum at 280.3 K is characterized by the quadrupole splitting $\Delta E_Q = 0.72 \pm 0.01 \text{ mm s}^{-1}$ and the isomer shift $\delta^{IS} = +0.92 \pm 0.01 \text{ mm s}^{-1}$ and thus corresponds to the high-spin 5T_2 ground state of iron(II). As the temperature is lowered, another doublet with a much larger value of the quadrupole splitting and a smaller value of the isomer shift appears, its intensity increasing at the expense of that of the first doublet. At 277.4 K, the two doublets have almost equal areas, whereas at 275.0 K, the relative contribution of the high-spin doublet has become very small. Finally, the lone doublet at 269.6 K is characterized by the Mössbauer parameters $\Delta E_Q = 1.64 \pm 0.01 \text{ mm s}^{-1}$ and $\delta^{IS} = +0.29 \pm 0.01 \text{ mm s}^{-1}$ and is assigned, particularly on the basis of the isomer shift value, to the low-spin 1A_1 ground state of iron(II). These observations thus indicate that the high-spin (5T_2) \rightleftharpoons low-spin (1A_1) transition in $[\text{Fe}(\text{phy})_2](\text{BF}_4)_2$ is quite sharp, being complete within a temperature range of less than 5.0 K. Detailed values of the Mössbauer parameters for a number of temperatures have been collected in Table I. If the measurements are followed for an increasing temperature sequence, the transition is found to be centered at $T_c^\dagger \approx 286 \text{ K}$, whereas the transition temperature for decreasing temperature measurements is significantly lower, being centered at $T_c^\dagger \approx 277 \text{ K}$. The transition is therefore associated with a thermal hysteresis, the width of the hysteresis loop being $\Delta T_c \approx 9 \text{ K}$.

From Figure 1, it is also apparent that the two quadrupole doublets corresponding to the high-spin 5T_2 and the low-spin 1A_1 phase show a slight intensity asymmetry of opposite direction. The intensity ratios assume the values $(I_\pi/I_\sigma)_{^1A_1} = 0.94$ and $(I_\pi/I_\sigma)_{^5T_2} = 1.14$, which are almost independent of temperature. These values apply over a wide temperature

Table I. ^{57}Fe Mössbauer-Effect Parameters of $[\text{Fe}(\text{phy})_2](\text{BF}_4)_2$ for a Set of Representative Temperatures in the Spin Transition Region

T, K	ΔE_{Q}^- ($^1\text{A}_1$), ^a mm s^{-1}	$\delta \text{IS}(^1\text{A}_1)$, ^b mm s^{-1}	ΔE_{Q}^- ($^5\text{T}_2$), ^a mm s^{-1}	$\delta \text{IS}(^5\text{T}_2)$, ^b mm s^{-1}	$A_{^5\text{T}_2}/A_{\text{total}}$
Increasing Temperatures					
246.0	1.64	+0.30			0
270.0	1.63	+0.29			0
280.8	1.62	+0.28			0
284.1	1.62	+0.28	0.68 ± 0.02	$+0.95 \pm 0.02$	0.14
285.6	1.63	+0.29	0.71	+0.94	0.31
286.3	1.61	+0.28	0.70	+0.93	0.42
287.1	1.61 ± 0.02	$+0.29 \pm 0.02$	0.71	+0.94	0.65
287.8	1.64 ± 0.02	$+0.30 \pm 0.02$	0.71	+0.94	0.82
288.5			0.71	+0.93	1.00
301.7			0.68	+0.92	1.00
320.4			0.62	+0.92	1.00
Decreasing Temperatures					
292.3			0.70	+0.93	1.00
287.6			0.71	+0.93	1.00
285.5			0.71	+0.94	1.00
280.3			0.72	+0.92	1.00
279.0			0.74	+0.93	0.93
278.2	1.66 ± 0.02	$+0.29 \pm 0.02$	0.75	+0.93	0.79
277.4	1.68	+0.30	0.77	+0.95	0.58
277.0	1.66	+0.28	0.77	+0.94	0.44
275.9	1.64	+0.28	0.72	+0.94	0.26
275.0	1.64	+0.28	0.72	+0.93	0.13
273.6	1.64	+0.28			0
260.9	1.64	+0.29			0
239.7	1.64	+0.31			0

^a Experimental uncertainty $\pm 0.01 \text{ mm s}^{-1}$ except where stated.

^b Isomer shifts δIS are listed relative to natural iron at 298 K. Experimental uncertainty $\pm 0.01 \text{ mm s}^{-1}$ except where stated.

region on either side of the spin transition. Thus it may be concluded that the observed asymmetry is due to texture and is not caused by the Goldanski-Karyagin effect. It should be noted, however, that significant and systematic deviations of I_{π}/I_{σ} from the above values are found in the spin transition region, for both the spin phases.

The temperature dependence of the isomer shift shows a considerable difference for the two spin phases. The resulting difference in the second-order Doppler shift conforms to the difference of Debye-Waller factors, since both quantities are interrelated. The results concerning the Debye-Waller factors will be discussed in detail in the next section.

In order to demonstrate the observed hysteresis effect, the area ratio for the high-spin $^5\text{T}_2$ ground state, $A_{^5\text{T}_2}/A_{\text{total}}$, has been plotted in the region of the spin transition, i.e. between 240 and 320 K, in Figure 2. The data in the figure apply to a single set of measurements, and these have been collected for an increasing, decreasing, and then a second increasing-temperature sequence, in this order, without disturbing the experimental arrangement. The figure shows that the transition temperature for the second increasing-temperature sequence is somewhat different from that in the first cycle of measurements, viz. $T_c^{\uparrow} \approx 284 \text{ K}$. A similar difference has been noticed also for the decreasing-temperature sequence.

Detailed ^{57}Fe Mössbauer-effect measurements have been also performed on another sample of the $[\text{Fe}(\text{phy})_2](\text{BF}_4)_2$ complex, which was prepared from natural iron. The resulting Mössbauer parameters are essentially identical with those of the enriched sample listed in Table I, and the transition is again complete at both temperature ends. However, the transition temperatures T_c^{\uparrow} and T_c^{\downarrow} for the second sample are slightly different from those reported above.

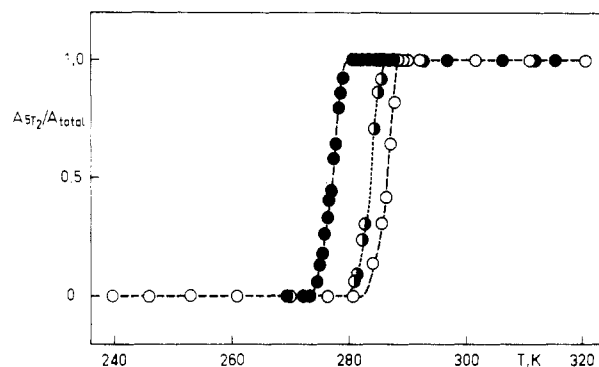


Figure 2. Temperature dependence of the high-spin area ratio $A_{^5\text{T}_2}/A_{\text{total}}$ for $[\text{Fe}(\text{phy})_2](\text{BF}_4)_2$ on the basis of Mössbauer-effect measurements. The data were collected for increasing (○), decreasing (●), and a second sequence of increasing (●) temperatures ($T_c^{\uparrow} \approx 286 \text{ K}$, $T_c^{\downarrow} \approx 277 \text{ K}$).

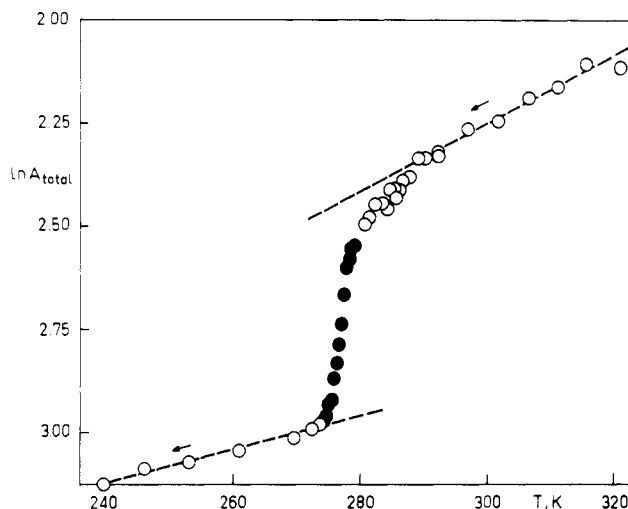


Figure 3. Temperature dependence of the quantity $-\ln A_{\text{total}}$ for a decreasing-temperature sequence for $[\text{Fe}(\text{phys})_2](\text{BF}_4)_2$. Open circles (○) correspond to temperatures where only one of the spin phases exists; filled circles (●) apply to the transition region where both phases coexist.

Quantities Derived from Mössbauer-Effect Areas. In Figure 3, the quantity $-\ln A_{\text{total}}$ is displayed, as derived from decreasing-temperature measurements. Beyond the spin transition region, the temperature function of $-\ln A_{\text{total}}$ is almost linear, whereas, at the spin transition temperature, a discontinuity is observed that arises due to the difference in the Debye-Waller factors for the two spin isomers, $-\ln f_{^5\text{T}_2}$ and $-\ln f_{^1\text{A}_1}$. From the slope of the two straight lines, the Debye temperatures for the two phases may be estimated. Assuming an effective mass $M_{\text{Fe}} = 57 \text{ au}$, values of $\Theta_{^5\text{T}_2} \approx 130 \text{ K}$ and $\Theta_{^1\text{A}_1} \approx 180 \text{ K}$ are obtained. From these, the difference in the recoil-free fractions, i.e. $\Delta f = (f_{^1\text{A}_1} - f_{^5\text{T}_2})/f_{^1\text{A}_1}$ at $T_c^{\downarrow} \approx 277 \text{ K}$ may be estimated as $\approx 65\%$. From Figure 3 it is also apparent that, on the high-temperature side, the quantity $-\ln A_{\text{total}}$ begins to deviate from the linear behavior considerably prior to the onset of the spin transition, and thus the rate of increase of the total area with decreasing temperature is somewhat higher than expected on the basis of the high-temperature approximation. Similar pretransitional effects have been observed for an increasing-temperature sequence of measurements.

It should be noted that, because of the difference in the Debye-Waller factors for the two phases, high-spin $^5\text{T}_2$ and low-spin $^1\text{A}_1$, the ratio $A_{^5\text{T}_2}/A_{\text{total}}$ used in Figure 2 does not represent exactly the high-spin fraction $n_{^5\text{T}_2}$. For the complex studied at present, this difference is particularly large due to the relatively high value of the transition temperature.

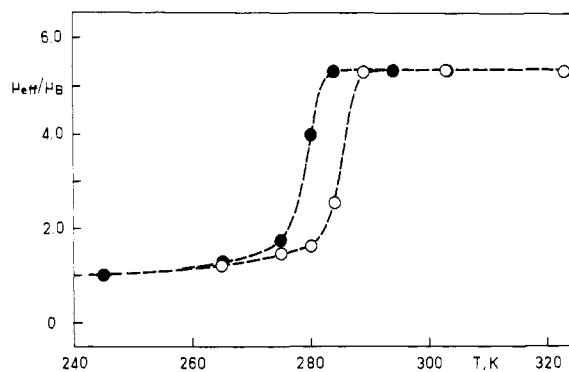


Figure 4. Temperature dependence of the effective magnetic moment μ_{eff} for $[\text{Fe}(\text{phy})_2](\text{BF}_4)_2$ for increasing (O) and decreasing (●) temperatures.

Table II. Magnetic Data for an Enriched Sample of $[\text{Fe}(\text{phy})_2](\text{BF}_4)_2^a$

T, K	$10^6 \times \chi_{\text{m}}^{\text{cor } b}$ cgs mol $^{-1}$	μ_{eff}^c μ_{B}	T, K	$10^6 \times \chi_{\text{m}}^{\text{cor } b}$ cgs mol $^{-1}$	μ_{eff}^c μ_{B}
89	450	0.59	323	10820	5.29
127	340	0.59	303	11540	5.29
166	275	0.60	294	11940	5.30
206	340	0.75	284	12250	5.28
265	680	1.20	280	7020	3.96
275	970	1.46	275	1370	1.74
280	1150	1.60	265	790	1.29
284	2810	2.52	245	520	1.01
289	12010	5.27	206	340	0.75
303	11540	5.29			

^a Data listed in the order of measurement. ^b Diamagnetic correction $\chi_{\text{m}}^{\text{dia}} = -432 \times 10^{-6}$ cgs mol $^{-1}$. ^c $\mu_{\text{eff}} = 2.828 \cdot (\chi_{\text{m}}^{\text{cor } b} T)^{1/2}$; experimental uncertainty approximately $\pm 0.02 \mu_{\text{B}}$.

Magnetic Measurements. The magnetism of the enriched sample of $[\text{Fe}(\text{phy})_2](\text{BF}_4)_2$ used for the Mössbauer-effect study has been measured between 89 and 323 K for both increasing- and decreasing-temperature sequences. At 323 K, the effective magnetic moment $\mu_{\text{eff}} = 5.29 \mu_{\text{B}}$ is characteristic of a high-spin ${}^5\text{T}_2$ ground state, whereas at 89 K $\mu_{\text{eff}} = 0.59 \mu_{\text{B}}$ implies a low-spin ${}^1\text{A}_1$ ground state. These values demonstrate again that the transition is practically complete at both temperature extremes. The detailed magnetic data are collected in Table II. Figure 4 illustrates the temperature dependence of μ_{eff} in the region of the transition. From the observed thermal hysteresis, the transition temperatures may be estimated as $T_c^\uparrow \approx 286 \text{ K}$ and $T_c^\downarrow \approx 279 \text{ K}$. These values are in very good agreement with the results of the Mössbauer-effect study. Three additional, independently prepared samples of $[\text{Fe}(\text{phy})_2](\text{BF}_4)_2$ have been studied by magnetic susceptibility measurements, and for all of these, a sharp spin transition with similar values of the transition temperatures and similar widths of the hysteresis loop have been obtained, whereas, due to the presence of small residual fractions, slight variations in μ_{eff} values have been encountered.

X-ray Powder Diffraction Studies. For the enriched sample of $[\text{Fe}(\text{phy})_2](\text{BF}_4)_2$, which was also used for the detailed Mössbauer-effect studies, X-ray diffraction patterns have been recorded in the region of the spin transition temperature, as described in the Experimental Section. The measurements were performed for values of the diffraction angle $3.5^\circ \leq \theta \leq 14.0^\circ$ and for both increasing- and decreasing-temperature sequences. Figure 5 shows three typical diffraction patterns at 282.8, 284.3, and 286.3 K for increasing temperature. From the figure it is evident that at the lowest temperature, i.e. 282.8 K, where the system is in the low-spin ${}^1\text{A}_1$ state, the diffraction pattern is significantly different from the pattern recorded at the highest temperature, i.e. 286.3 K, where the system is in

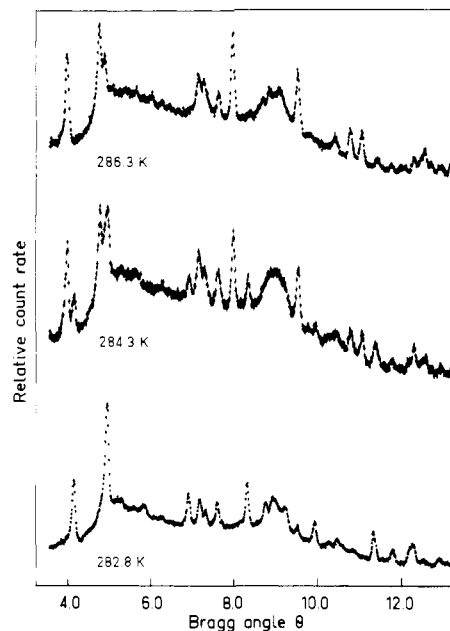


Figure 5. X-ray powder diffraction patterns of $[\text{Fe}(\text{phy})_2](\text{BF}_4)_2$ at 282.8, 284.3, and 286.3 K. The measurements refer to increasing-temperature measurements.

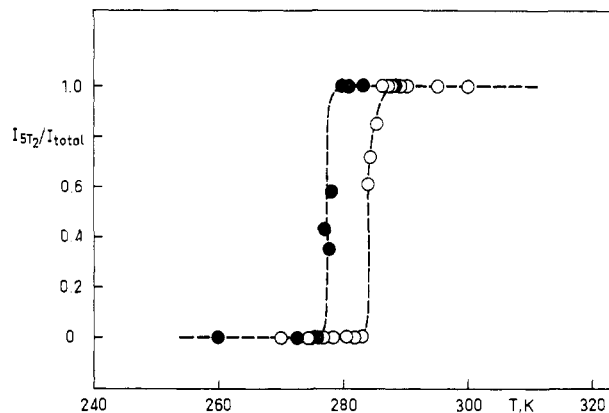


Figure 6. Temperature dependence of the relative intensity of the high-spin phase $I_{5\text{T}_2}/I_{\text{total}}$ for $[\text{Fe}(\text{phy})_2](\text{BF}_4)_2$ on the basis of X-ray powder diffraction measurements. The data were collected for increasing- (O) and decreasing- (●) temperature sequences.

the high-spin ${}^5\text{T}_2$ state. For intermediate temperatures, e.g. 284.3 K, the diffraction pattern may be easily understood as a superposition of the two patterns for the pure ground states with a temperature-dependent relative intensity. The observations imply a crystallographic phase change that occurs either at the same temperature as the spin transition or at a temperature in close proximity. For the decreasing-temperature sequence, the phase transition takes place at a somewhat lower temperature.

In order to describe the progress of the phase transition on a quantitative basis, the diffraction peak profiles for two corresponding well-resolved Bragg reflections situated at $\theta = 4.156^\circ$ for the low-spin ${}^1\text{A}_1$ state and at $\theta = 3.995^\circ$ for the high-spin ${}^5\text{T}_2$ state have been studied with use of an angular step of 0.005° for the 2θ values. Accurate values for the peak position and the intensity ratio $R = I_{5\text{T}_2}/(I_{5\text{T}_2} + I_{1\text{A}_1})$ have been obtained by a least-squares fit to Gaussian line shape. In Figure 6, the intensity ratio R is displayed as a function of temperature for both increasing- and decreasing-temperature sequences. From the figure it is seen that the phase transition is complete at both extremes of the temperature range, the transition temperature being $T_c^\uparrow \approx 284 \text{ K}$ for the increasing-temperature sequence and $T_c^\downarrow \approx 277 \text{ K}$ for the de-

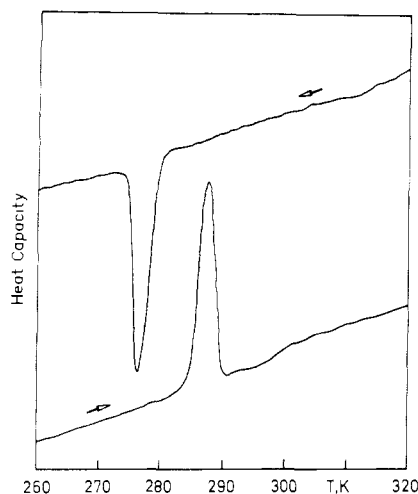


Figure 7. DSC curves for $[\text{Fe}(\text{phy})_2](\text{BF}_4)_2$ for increasing- and decreasing-temperature sequences. Sample weight is 6.90 mg. Arrows indicate the direction of temperature variation.

ing-temperature sequence. The width of the hysteresis loop then follows as $\Delta T_c \approx 7$ K. It should be noted that, in view of the considerable difference in intensity of the two selected peaks and the difference of Debye–Waller factors for the two phases, the intensity ratio R does not represent exactly the relative fractions of the two phases.

Differential Scanning Calorimetry. Figure 7 shows the DSC curves for one of the samples of $[\text{Fe}(\text{phy})_2](\text{BF}_4)_2$ for both an increasing- and a decreasing-temperature sequence. For increasing temperatures, an endothermic peak corresponding to the transformation ${}^1A_1 \rightarrow {}^5T_2$ starts to build up around 285 K, its maximum being centered at $T_c^\dagger \approx 288$ K. For decreasing temperatures, an exothermic peak corresponding to the ${}^5T_2 \rightarrow {}^1A_1$ transformation starts to appear at about 280 K with the maximum at $T_c^\dagger \approx 276$ K. Thus the hysteresis effects reported above are reproduced in DSC quite well. The slight differences for the values of transition temperatures and for the width of thermal hysteresis may arise due to the different mode of thermal equilibrium, which is dynamic in DSC. The enthalpy change associated with the spin transition has been derived as $\Delta H = 24.2 \pm 1.0$ kJ mol $^{-1}$ and the entropy change as $\Delta S = 85.8 \pm 4.0$ J mol $^{-1}$ K $^{-1}$ if the true thermodynamic transition temperature is taken as $T_c = 282$ K, which is the average of the observed two values.

Effect of Pressure on the ${}^5T_2 \rightarrow {}^1A_1$ Transformation. The enriched sample of $[\text{Fe}(\text{phy})_2](\text{BF}_4)_2$ was selected to test the possibility of inducing the high-spin (5T_2) \rightarrow low-spin (1A_1) transformation by the application of pressure. It has been demonstrated above (cf. Table I) that, in the ${}^{57}\text{Fe}$ Mössbauer effect at 288.5 K and atmospheric pressure, the sample showed only the characteristic doublet of the high-spin 5T_2 ground state. When the moderate pressure of 0.6 or 1.2 kbar was applied, a superposition of the spectra of the two spin phases was observed. Figure 8 shows the Mössbauer spectra of the sample at 296.6 K under ambient pressure and the pressure of 1.2 kbar. The values derived for the area fraction of the two spectra are $A_{{}^5T_2}/A_{\text{total}} = 1.0$ at $p = 1$ bar, 0.64 at $p = 0.6$ kbar, and 0.58 at $p = 1.2$ kbar. The values for the quadrupole splitting and the isomer shift of the pressure-induced low-spin 1A_1 state, viz. $\Delta E_Q = 1.63$ mm s $^{-1}$ and $\delta^{1S} = +0.30$ mm s $^{-1}$, are in excellent agreement with the values obtained for the temperature-induced 1A_1 phase. The detailed values for the Mössbauer parameters at the pressures of 0.6 and 1.2 kbar are listed in Table III.

Discussion

Nature of the High-Spin (5T_2) \rightleftharpoons Low-Spin (1A_1) Transition. According to the conventional thermodynamic classification,¹⁶

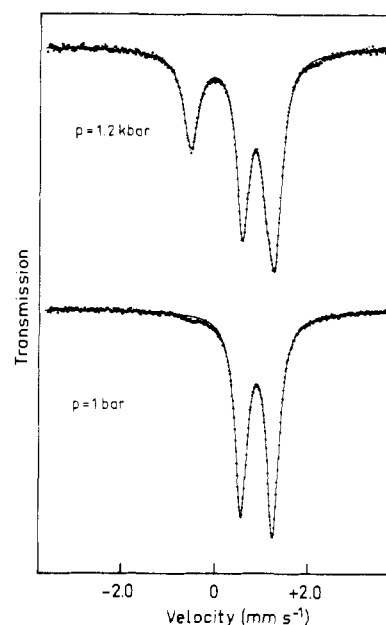


Figure 8. ${}^{57}\text{Fe}$ Mössbauer-effect spectra for an enriched sample of $[\text{Fe}(\text{phy})_2](\text{BF}_4)_2$ at 296.6 K at the pressure of 1.20 kbar and at ambient pressure.

Table III. ${}^{57}\text{Fe}$ Mössbauer-Effect Parameters for Pressure-Induced Spin Transition in $[\text{Fe}(\text{phy})_2](\text{BF}_4)_2$ at 296.6 K

P , kbar	ΔE_Q^- (1A_1), mm s $^{-1}$	δ^{1S} (1A_1), mm s $^{-1}$	ΔE_Q^- (5T_2), mm s $^{-1}$	δ^{1S} (5T_2), mm s $^{-1}$	$A_{{}^5T_2}/$ A_{total}
0.001			0.68	+0.93	1.00
0.60	1.62	+0.27	0.69	+0.91	0.64
1.20	1.63	+0.30	0.70	+0.95	0.58

a transition is first order if discontinuous changes of volume and entropy are observed. For $[\text{Fe}(\text{phy})_2](\text{BF}_4)_2$, these conditions are well established by the observations reported above. Thus the formation of individual X-ray diffraction patterns for the two spin states, 5T_2 and 1A_1 , is clear evidence for a crystallographic phase change; the latter is associated with a change in volume. The results of Mössbauer spectroscopy provide independent support for the first-order character of the transition. Thus a discontinuous change of the quantity $-\ln A_{\text{total}}$ has been observed (cf. Figure 3), which is directly related to the Debye–Waller factor $-\ln f_{\text{total}}$. The large difference in the Debye temperatures $\Theta_{{}^5T_2}$ and $\Theta_{{}^1A_1}$ derived therefrom implies corresponding differences in the phonon spectrum for the two lattices; the latter are likely the result of a change in volume. Finally, a change in entropy of $\Delta S = 85.8$ J mol $^{-1}$ K $^{-1}$ is clearly indicated by the results of the DSC study. Thus it is clear that the observed high-spin (5T_2) \rightleftharpoons low-spin (1A_1) transition in $[\text{Fe}(\text{phy})_2](\text{BF}_4)_2$ is associated with a crystallographic phase change and is first order.

Moreover, the transition temperatures derived from Mössbauer-effect measurements (viz. $T_c^\dagger \approx 286$ K, $T_c^\dagger \approx 277$ K), X-ray diffraction measurements (viz. $T_c^\dagger \approx 284$ K, $T_c^\dagger \approx 277$ K), and DSC (viz. $T_c^\dagger \approx 288$ K, $T_c^\dagger \approx 276$ K) are in close agreement. It is therefore believed that the spin transition and the crystallographic phase change occur concomitantly. It is very likely that the phase change effectively triggers the spin transition. This is indicated by the observation of pretransitional effects, which have been derived from Mössbauer spectra, in particular from the temperature dependence of $-\ln A_{\text{total}}$. Most likely, these effects are associated

(16) P. Ehrenfest, *Commun. Kamerlingh Onnes Lab. Univ. Leiden, Suppl.*, No. 36, 153 (1933).

with the softening of a certain vibrational mode which is responsible for the transition.

It should be noted that it has not been possible to derive values of the high-spin fraction n_{5T_2} from Mössbauer-effect areas. The deviations of $-\ln A_{\text{total}}$ clearly show that the iterative procedure⁶ cannot be applied to the present results.

An additional characteristic of first-order phase transitions is thermal hysteresis, which has therefore often been employed as an indication for this type of transition. For $[\text{Fe}(\text{phy})_2](\text{BF}_4)_2$, a pronounced hysteresis of width $\Delta T_c \approx 7$ K has indeed been found, consistent results being provided by four independent physical methods, i.e. ⁵⁷Fe Mössbauer-effect, magnetic susceptibility, DSC, and X-ray diffraction measurements. In compounds of iron(II), hysteresis effects associated with spin transitions have been previously reported for $[\text{Fe}(4,7-(\text{CH}_3)_2\text{phen})_2(\text{NCS})_2]$ (phen = 1,10-phenanthroline),^{11,17} $[\text{Fe}(\text{paptH})_2](\text{NO}_3)_2$ (paptH = 2-(2-pyridylamino)-4-(2-pyridyl)thiazole),¹⁸ $[\text{Fe}(2\text{-pic})_3]\text{Cl}_2 \cdot \text{H}_2\text{O}$ (2-pic = 2-picolylamine),¹⁹ $[\text{Fe}(\text{bt})_2(\text{NCS})_2]$ (bt = 2,2'-bi-2-thiazoline),¹⁰ $[\text{Fe}(\text{phy})_2](\text{ClO}_4)_2$,⁹ and $[\text{Fe}(\text{bi})_3](\text{ClO}_4)_2$ (bi = 2,2'-bi-2-imidazoline).¹² Recently, a very narrow hysteresis of $\Delta T_c = 0.15$ K has been detected^{20,21} for $[\text{Fe}(\text{phen})_2(\text{NCS})_2]$ (extracted sample), a system for which the nature of the transition was somewhat obscure;²² in addition, $\Delta T_c \approx 0.4$ K has been reported²⁰ for $[\text{Fe}(\text{bpy})_2(\text{NCS})_2]$.

The DSC results obtained for $[\text{Fe}(\text{phy})_2](\text{BF}_4)_2$ are of large significance in establishing the first-order character of the spin transition for this compound. The only other system for which values of ΔH and ΔS have been obtained on the basis of calorimetric measurements²³ is $[\text{Fe}(\text{phen})_2(\text{X})_2]$, where X = NCS or NCSe. It should be noted that the values for the present complex, i.e. $\Delta H = 24.2$ kJ mol⁻¹ and $\Delta S = 85.8$ J mol⁻¹ K⁻¹, are significantly larger than the corresponding values for $[\text{Fe}(\text{phen})_2(\text{NCS})_2]$, viz. $\Delta H = 8.6$ kJ mol⁻¹ and $\Delta S = 48.78$ J mol⁻¹ K⁻¹, or those for $[\text{Fe}(\text{phen})_2(\text{NCSe})_2]$, viz. $\Delta H = 11.60$ kJ mol⁻¹ and $\Delta S = 51.22$ J mol⁻¹ K⁻¹.²³ This suggests that the structural changes associated with the spin transition in the present complex are more pronounced than those in the $[\text{Fe}(\text{phen})_2(\text{X})_2]$ system. The entropy change is also significantly larger than the value of $\Delta S_{\text{spin}} = R \ln(2S + 1) = 13.4$ J mol⁻¹ K⁻¹, which results from the change in the spin state of the complex. The additional contribution to the entropy change beyond ΔS_{spin} is due to the change in the phonon spectrum of the compound, which is also reflected in the quantities derived from the Mössbauer-effect studies.

The temperature $T_0 = 1/2(T_c^{\uparrow} + T_c^{\downarrow}) \approx 281.5$ K, at which the free energies of the two phases are equal, is the true thermodynamic phase transition temperature. However, at this temperature T_0 , it is not possible to have any sustained nucleation and phase growth of the transformed phase.²⁴ In order that the phase transition proceed, slight superheating or supercooling is essential for the increasing- or decreasing-temperature sequence, respectively. This relation gives rise to the observed thermal hysteresis in first-order phase transitions. The formation of the nuclei of the secondary phase is caused by fluctuations due to thermal agitation. In general,

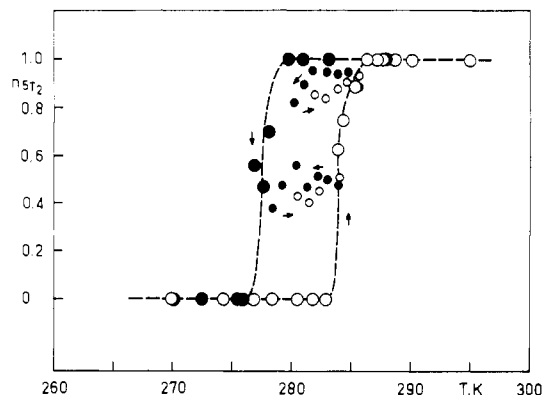


Figure 9. Temperature dependence of the high-spin fraction n_{5T_2} for $[\text{Fe}(\text{phy})_2](\text{BF}_4)_2$ derived on the basis of X-ray diffraction measurements. The data are for increasing- (○) and decreasing- (●) temperature sequences. The two scanning curves were obtained for the temperature difference of $\Delta T = 5.5$ K. Arrows indicate the direction of temperature variation.

defect sites are the preferred sites for the precipitation of the nuclei. Because of the strong cooperative interaction between the molecules in the lattice, the nuclei grow farther across the interface to form the domains of the transformed phase. When the size of these domains exceeds a certain critical value, they give rise to the characteristic X-ray diffraction pattern of the transformed phase. On the basis of the present results it is believed that, when the temperature is varied slightly in the phase transition region, the equilibrium concentration of the two phases is attained within a few minutes. These conclusions are based on the observation of constant area ratios $A_{5T_2}/A_{\text{total}}$ obtained from Mössbauer spectra recorded over both a short interval and an extended period of time at the one temperature.

Attempt at Application of the Everett Model. Detailed studies of hysteresis effects, in particular the construction of multiple inner scanning curves, may provide quite specific information with regard to the mechanism of phase transitions if the theorems of Everett²⁵⁻²⁷ are applied. This has been recently verified for the analogous complex $[\text{Fe}(\text{phy})_2](\text{ClO}_4)_2$ using data from the X-ray powder diffraction measurements. The parameter employed in that study was the intensity ratio $R = I_{5T_2}/(I_{5T_2} + I_{A_1})$, which was averaged over four different Bragg reflections. However, the quantity to be applied is the actual high-spin fraction n_{5T_2} rather than R . For a powder pattern, n_{5T_2} may be obtained from the intensity ratio R according to¹⁴

$$n_{5T_2} = \frac{R}{R + \alpha(1 - R)} \quad (1)$$

Here, $\alpha = I_{5T_2}^0/I_{A_1}^0$, where $I_{5T_2}^0$ and $I_{A_1}^0$ are the intensities of the selected Bragg reflections at the beginning and at the end of the phase transition. In general, the quantity α should show a temperature dependence due to the difference of Debye-Waller factors for the two phases. As a first approximation, the temperature dependence of α over the spin transition region can be neglected for the present system because of the sharp nature of the transition. The temperature dependence of n_{5T_2} shown in Figure 9 has been obtained from the X-ray powder diffraction data according to eq 1. In the figure, n_{5T_2} is plotted for the main hysteresis curve as well as for two inner scanning curves, which have been obtained by appropriate interruption of the increasing-temperature branch. The scanning curves apply to the temperature intervals 278.4

(17) E. König and G. Ritter, *Solid State Commun.*, **18**, 279 (1976).

(18) G. Ritter, E. König, W. Irlner, and H. A. Goodwin, *Inorg. Chem.*, **17**, 224 (1978).

(19) M. Sorai, J. Ensling, K. M. Hasselbach, and P. Gütllich, *Chem. Phys.*, **20**, 197 (1977).

(20) E. W. Müller, H. Spiering, and P. Gütllich, *Chem. Phys. Lett.*, **93**, 567 (1982).

(21) P. Ganguli, P. Gütllich, and E. W. Müller, *Inorg. Chem.*, **21**, 3429 (1982).

(22) P. Ganguli, P. Gütllich, and E. W. Müller, *J. Chem. Soc., Dalton Trans.*, 441 (1981).

(23) M. Sorai, and S. Seki, *J. Phys. Chem. Solids*, **35**, 555 (1974).

(24) C. N. R. Rao and K. J. Rao, "Phase Transitions in Solids", McGraw-Hill, New York, 1978.

(25) D. H. Everett and W. I. Whitton, *Trans. Faraday Soc.*, **48**, 749 (1952).

(26) D. H. Everett and F. W. Smith, *Trans. Faraday Soc.*, **50**, 187 (1954).

(27) D. H. Everett, *Trans. Faraday Soc.*, **50**, 1077 (1954); **51**, 1551 (1955).

$K \leq T \leq 283.9$ K and 280.1 K $\leq T \leq 285.6$ K, their width being 5.5 K in both cases. The slopes of the scanning curves are not well-defined, and unlike the results for $[\text{Fe}(\text{phy})_2](\text{ClO}_4)_2$, they are not suitable for the application of the model suggested by Everett. In an attempt to test theorem 4 of Everett, which refers to the noninteracting nature of the domains, the inner loops were constructed by interrupting the temperature in both the increasing and the decreasing branch and recording the scanning curves for the same temperature interval; but again, unsuitable results were obtained. The problems encountered here seem to be due to the slightly nonreproducible character of the intensities of X-ray diffraction in the spin transition region (cf. Figure 2). It has been generally found¹⁴ that, for many systems exhibiting hysteresis effects, the crystallites crack in the process of the multiple cycling of temperature over the phase transition region. This behavior is most likely caused by the strains that develop in the system. The cracking leads to additional defects, which result in a variation of the values for T_c and ΔT_c , ultimately producing the overall differences observed. At any rate, the present results show that a distribution of both T_c and ΔT_c values exists, since a constant value of ΔT_c would not allow the appearance of an area enclosed by the scanning curves.

The much more satisfactory results for the complex $[\text{Fe}(\text{phy})_2](\text{ClO}_4)_2$ were achieved⁹ apparently because the intensity ratio R was averaged over four different peaks. In this way, the experimental errors that give rise to the scatter of the individual n_{5T_2} values in Figure 8 will have been averaged as well. In the present case, this procedure cannot be applied since only a single well-defined diffraction peak is available.

Pressure-Induced High-Spin (5T_2) \rightarrow Low-Spin (1A_1) Transformation. The present results show that, in $[\text{Fe}(\text{phy})_2](\text{BF}_4)_2$, a transition between the ground states high-spin 5T_2 and low-spin 1A_1 may be effected by application of a rather moderate pressure, viz. 0.6 or 1.2 kbar. Apparently, this pressure exerts a large enough lattice strain such as to induce a transformation to the state of lower molecular volume. No definite evidence concerning the thermodynamic nature of the transformation is available at this time. However, the transformed phase in the low-spin 1A_1 state should be closely similar to the low-spin phase induced by temperature variation. This conclusion is supported by the close agreement of the corresponding values of the Mössbauer parameters $\Delta E_Q(^1A_1)$ and $\delta^{57}\text{Fe}(^1A_1)$ for the two phases. Pressure-induced conversions between the high-spin and low-spin phases in complexes of iron(II) have been reported previously. Thus Drickamer and co-workers^{28,29} studied, in particular, the classical spin-crossover

complexes $[\text{Fe}(\text{phen})_2(\text{NCS})_2]$ and $[\text{Fe}(\text{phen})_2(\text{NCSe})_2]$ as well as various related iron(II) complexes of 1,10-phenanthroline. Recently, Long et al.³⁰ reported a pressure-induced transformation in $[\text{Fe}[\text{HB}(3,5\text{-Me}_2\text{pz})_3]_2]$, where $\text{HB}(3,5\text{-Me}_2\text{pz}) = \text{hydrotris}(3,5\text{-dimethyl-1-pyrazolyl})\text{borate}$. In these investigations, considerably higher pressure ranges have been employed than in the present study. Only very recently has the effect of low pressure on the spin transition in $[\text{Fe}(\text{2-pic})_3]\text{Cl}_2 \cdot \text{C}_2\text{H}_5\text{OH}$ been communicated.³¹

Unusual Values of the Quadrupole Splitting. The unusual values of the quadrupole splitting for the $[\text{Fe}(\text{phy})_2](\text{BF}_4)_2$ complex, i.e. the relatively small value of $\Delta E_Q(^5T_2)$ and the relatively large value of $\Delta E_Q(^1A_1)$, are attributed to the unsymmetrical nature of the ligand and the distortion created by the tridentate coordination of the ligands at the iron(II) site. The situation seems to be largely similar to that in the iron(II) complexes of the 4-paptH⁷ and pythiaz³² ligands, where pythiaz = 2,4-bis(2-pyridyl)thiazole. For these complexes, the unusually large $\Delta E_Q(^1A_1)$ is practically independent of temperature, whereas $\Delta E_Q(^5T_2)$ shows a significant temperature dependence. This suggests that the temperature-independent $\Delta E_Q(^1A_1)$ is arising mainly due to highly asymmetric lattice charges, whereas in $\Delta E_Q(^5T_2)$ this contribution is partly compensated by the temperature-dependent valence contribution for the high-spin 5T_2 phase, thereby producing the relatively small value of ΔE_Q that is ultimately observed.

Remark concerning the Effect of the Anion. It may be of some interest that the anion replacement in $[\text{Fe}(\text{phy})_2](\text{ClO}_4)_2$ by the BF_4^- anion has very little effect on the discontinuous nature of the transition. A similar observation has been made for the continuous type of spin transition in the complexes $[\text{Fe}(4\text{-paptH})_2]\text{X}_2 \cdot 2\text{H}_2\text{O}$, where $\text{X} = \text{ClO}_4^-, \text{BF}_4^-$.⁷ In both cases, the value of the transition temperature T_c increases slightly with the replacement of ClO_4^- by BF_4^- : for the complexes of phy, $T_c^1 \approx 256$ and 286 K, whereas for those of 4-paptH, $T_c \approx 185$ and 220 K, respectively. This variation may arise from the electronegativity difference of the anions, ClO_4^- and BF_4^- , which will produce, through the surrounding ligands, a slight change in the crystal field strength at the site of the iron(II) ion.

Acknowledgment. We appreciate financial support by the Stiftung Volkswagenwerk and the Fonds der Chemischen Industrie.

Registry No. $[\text{Fe}(\text{phy})_2](\text{BF}_4)_2$, 53261-61-3.

(28) C. B. Barger and H. G. Drickamer, *J. Chem. Phys.*, **55**, 3471 (1971).

(29) C. W. Frank and H. G. Drickamer, *J. Chem. Phys.*, **56**, 3551 (1972).

(30) G. J. Long, L. W. Becker, and B. B. Hutchinson, *Adv. Chem. Ser.*, No. **194**, 453 (1981).

(31) E. Meissner, H. Köppen, H. Spiering, and P. Gülich, *Chem. Phys. Lett.*, **95**, 163 (1983).

(32) E. König, G. Ritter, and H. A. Goodwin, *Chem. Phys.*, **1**, 17 (1973).